Hindawi Publishing Corporation
Advances in Materials Science and Engineering
Volume 2015, Article ID 146476, 5 pages
http://dx.doi.org/10.1155/2015/146476

Research Article

Effect of Nanosized NiF_2 Addition on the Transport Critical Current Density of Ag-Sheathed $(Bi_{1.6}Pb_{0.4})Sr_2Ca_2Cu_3O_{10}$ Superconductor Tapes

M. Hafiz and R. Abd-Shukor

School of Applied Physics, Universiti Kebangsaan Malaysia, 43600 Bangi, Selangor, Malaysia

Correspondence should be addressed to R. Abd-Shukor; ras@ukm.edu.my

Received 17 November 2014; Accepted 6 January 2015

Academic Editor: Sanjeeviraja Chinnappanadar

We report the effect of NiF_2 (10 nm) additions on the transport critical current density, J_c of $(Bi_{1.6}Pb_{0.4})Sr_2Ca_2Cu_3O_{10}$/Ag sheathed superconductor tapes. Pellets of $(Bi_{1.6}Pb_{0.4})Sr_2Ca_2Cu_3O_{10}(NiF_2)_x$ (x = 0–0.05 wt.%) superconductor were prepared using the acetate coprecipitation method. The sample with 0.04 wt.% addition of NiF_2 exhibited the highest J_c. Ag-sheathed $(Bi_{1.6}Pb_{0.4})Sr_2Ca_2Cu_3O_{10}(NiF_2)_{0.04}$ superconductor tapes were fabricated using the powder-in-tube (PIT) method and sintered at 845°C for 50 and 100 h. J_c of nonadded tapes at 30 K sintered for 50 and 100 h was 6370 and 8280 A/cm^2, respectively. J_c of $(Bi_{1.6}Pb_{0.4})Sr_2Ca_2Cu_3O_{10}(NiF_2)_{0.04}$/Ag tape at 30 K sintered for 50 and 100 h was 14390 and 17270 A/cm^2, respectively. In magnetic fields (0 to 0.7 T), J_c of the NiF_2 added tapes was also higher compared with the nonadded tape indicating that NiF_2 nanoparticles can act as effective flux pinning centers and longer sintering time improved the microstructure. A steeper increase in J_c was observed below 60 K in the NiF_2 added tapes which coincided with the Neel temperature, T_N of nanosized NiF_2 (60 K). The pronounced enhancement of J_c was attributed to the strong interaction between flux line network and the antiferromagnetic NiF_2 below T_N.

1. Introduction

The $Bi_{1.4}Pb_{0.6}Sr_2Ca_2Cu_3O_{10+\delta}$ (Bi-2223) high temperature superconductor shows great potential for commercialization in various applications. However, weak pinning of flux lines and weak intergrain links result in low transport critical current density, J_c, especially in magnetic fields and these limit the application of this material [1, 2]. In order to improve the flux pinning, several methods such as adding impurities to act as pinning centers have been employed. Additions of particles such as TiO_2, ZrO_2, Ag_2CO_3, and MgO in Bi-2223 have been investigated and shown to increase the transport critical current density [3–6].

Furthermore, addition of magnetic nanoparticles to enhance J_c in Bi-2223 has also been proposed. If the average size of the nanoparticles, d, is $\xi < d < \lambda$, where ξ is the coherence length and λ is the penetration depth, an increase in J_c can be expected due to enhanced flux pinning which arises from strong interaction between flux line network and magnetic system in the superconductor [7]. Previous studies with magnetic nanoparticles such as $NiFe_2O_4$ and Fe_3O_4 addition to Bi-2223 have also showed improvements in the transport properties [8, 9].

The coherence length of Bi-2223 is around 2.9 nm and the penetration depth is between 60 and 1000 nm [10]. The average size of NiF_2 nanoparticles employed in this study is 10 nm that is between the coherence length and penetration depth of Bi-2223. This satisfies the requirement for a frozen flux superconductor [7]. NiF_2 nanoparticle has a rutile crystal structure and the Néel temperature is 60 K [11]. It is interesting to investigate the J_c of Bi-2223 added with nano NiF_2 above and below 60 K where the magnetic transition occurs. The objectives of this study were to investigate the effect of NiF_2 nanoparticles with average size of 10 nm on the structure, phase formation, and transport critical current density of Ag-sheathed Bi-2223 tapes with different sintering times.

Table 1: Volume fraction and critical current density (at 30 K and 77 K) of $x = 0$ and 0.04 wt.% of 10 nm NiF_2 added Bi-2223 tapes sintered for 50 and 100 h.

x (wt.%)	Sintering time (h)	Volume fraction		J_c (A/cm^2) at 30 K	J_c (A/cm^2) at 77 K
		Bi-2223	Bi-2212		
0.00	50	73	27	6370	1040
0.00	100	76	24	8280	1290
0.04	50	84	16	14390	3090
0.04	100	85	15	17270	3730

2. Experimental Details

$Bi_{1.4}Pb_{0.6}Sr_2Ca_2Cu_3O_{10}$ superconductor pellets were prepared by the acetate coprecipitation method [12]. Nanosized NiF_2 (Aldrich, 99.99% purity) with 10 nm average size was added with composition $(Bi_{1.6}Pb_{0.4})Sr_2Ca_2Cu_3O_{10}(NiF_2)_x$ (x = 0.00–0.05 wt.%). The mixed powders were ground and pressed into pellets and then sintered at 845°C for 48 h. The sample with $x = 0.04$ wt.% showed the highest J_c at 77 K. This composition was chosen to fabricate Ag-sheathed tape by the powder-in-tube method. $(Bi_{1.6}Pb_{0.4})Sr_2Ca_2Cu_3O_{10}(NiF_2)_{0.04}$ powders were packed into a 6.35 mm outer diameter and 4.35 inner diameter Ag tube (Alfa Aesar, 99.9%). The tube was drawn to a 1 mm wire and then pressed into 0.12 nm thick and 1.35 nm wide tapes. The tapes were then cut into 2-3 cm sections and sintered for 50 h and 100 h at 845°C. Tapes without the addition of NiF_2 were also prepared for comparison.

The J_c of the tapes was measured using the four-point probe method with the 1 μV/cm criterion. The measurements were done from 30 K to 77 K in zero fields and at 77 K under magnetic field from 0 to 0.75 T. X-ray diffraction (XRD) patterns of the tapes were recorded using a Bruker D8 Advance diffractometer with CuK_α radiation. The Ag sheath was removed prior to measurement. The microstructure of the tapes was examined using a Philips XL 30 scanning electron microscope. A Philips transmission electron microscope (model CM12) was used to confirm the average size of NiF_2 nanoparticles.

3. Results and Discussion

NiF_2 added Bi-2223 pellet with $x = 0.04$ wt.% showed the highest J_c of 2.54 and 1.38 A/cm^2 at 30 K and 77 K, respectively (Figure 1). This optimal wt.% was used to prepare $(Bi_{1.6}Pb_{0.4})Sr_2Ca_2Cu_3O_{10}(NiF_2)_{0.04}$/Ag tape.

Figure 2 shows the XRD patterns of $x = 0$ and 0.04 wt.% tapes sintered for 50 and 100 h. Most of the peaks in both nonadded and NiF_2 added tapes belong to the high-T_c phase (Bi-2223) with a few peaks corresponding to the low-T_c phase (Bi-2212). The volume fraction of Bi-2223 phase was calculated using

$$V_{2223} = \frac{\sum I_{2223}}{\sum I_{2223} + \sum I_{2212}}, \quad (1)$$

where $\sum I_{2223}$ and $\sum I_{2212}$ are the sum of intensities of Bi-2223 and Bi-2212 phase, respectively [13, 14]. The volume fractions are shown in Table 1. In general, the Bi-2223 peaks increased with NiF_2 addition and with longer sintering times. The tape sintered for 100 h showed the highest volume fraction.

Figure 3(a) shows the TEM micrograph of the NiF_2 nanoparticles employed in this study with average grain

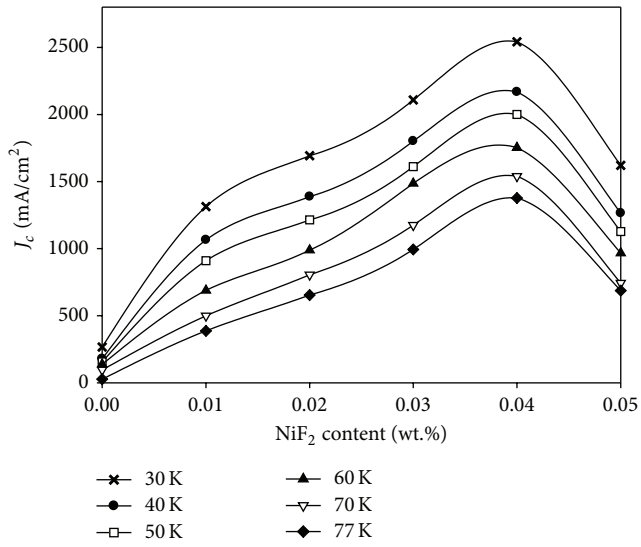

Figure 1: Critical current density, J_c, of Bi-2223 pellets as function of wt.% NiF_2 content between 30 K and 77 K.

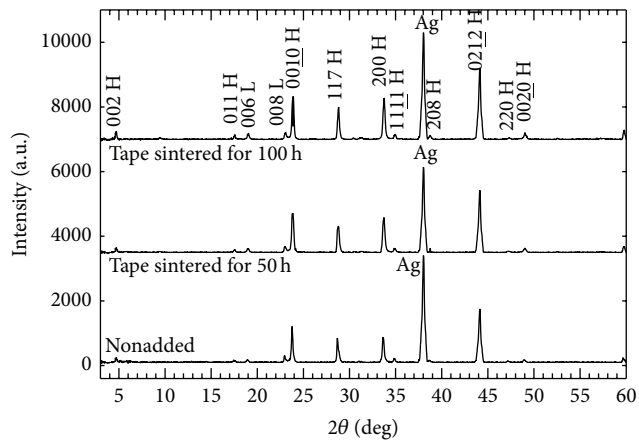

Figure 2: XRD patterns of nonadded and NiF_2 nanoparticle added tapes sintered for 50 and 100 h. (H) denotes the high-T_c phase (Bi-2223) and (L) denotes the low-T_c phase (Bi-2212).

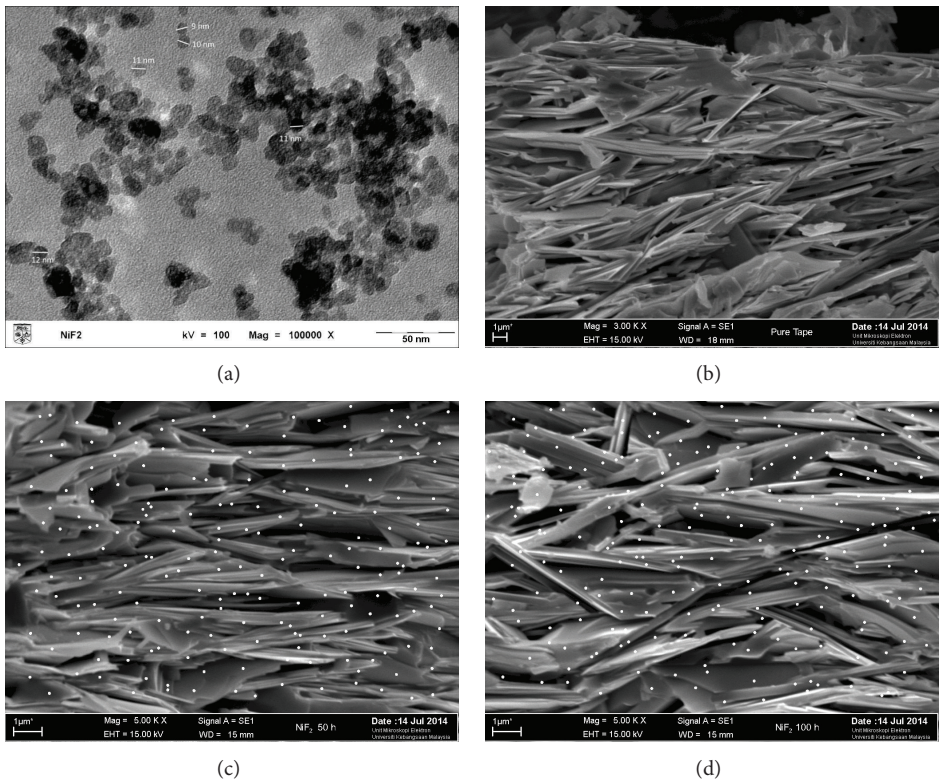

Figure 3: Micrographs of (a) NiF_2 with average size 10 nm, (b) nonadded Bi-2223 tape, (c) NiF_2 added Bi-2223 tape sintered for 50 h, and (d) NiF_2 added Bi-2223 tape sintered for 100 h. White dots denote the distribution of NiF_2 nanoparticle in the tapes.

size of 10 nm. SEM micrographs of nonadded and NiF_2 added tapes in Figures 3(b)–3(d) showed plate-like grains microstructure which is the typical microstructure of the Bi-2223 system. Figures 3(c) and 3(d) also show the distribution of NiF_2 (white dots).

J_c of nonadded and NiF_2 added tapes sintered for 50 and 100 h in zero fields is shown in Figure 4. Tapes with NiF_2 addition showed significantly higher J_c compared with the nonadded tapes. Furthermore, longer sintering times also contributed to a slight increase of J_c in both nonadded and NiF_2 added tapes. This could be due to improvement in connectivity between grains with longer sintering times. J_c of all tapes decreased with an increase in temperature as a consequence of thermally activated flux creep. J_c of NiF_2 added tape sintered for 100 h was 17270 A/cm^2 at 77 K, which is higher than J_c of the tape sintered for 50 h (14390 A/cm^2) as shown in Table 1. However, the J_c is lower compared with nanosized PbO, Fe_3O_4, and MgO added Ag-sheathed Bi-2223 tapes sintered for 100 h (26800 A/cm^2, 23130 A/cm^2, and 18380 A/cm^2, resp., at 30 K), but higher than J_c of NiO added Bi-2223 tapes (15520 A/cm^2 at 30 K) [9, 15–17].

Below 60 K, the J_c of NiF_2 added tapes showed a steeper increase (Figure 4) which coincides with the Néel temperature, T_N = 60 K of NiF_2 [11]. The appearance of antiferromagnetism in NiF_2 below 60 K may have been the cause of the steeper increase in J_c as suggested in a frozen flux superconductor [7].

Magnetic field dependence of J_c for the nonadded and NiF_2 added tapes at 77 K from 0 T to 0.75 T with the applied

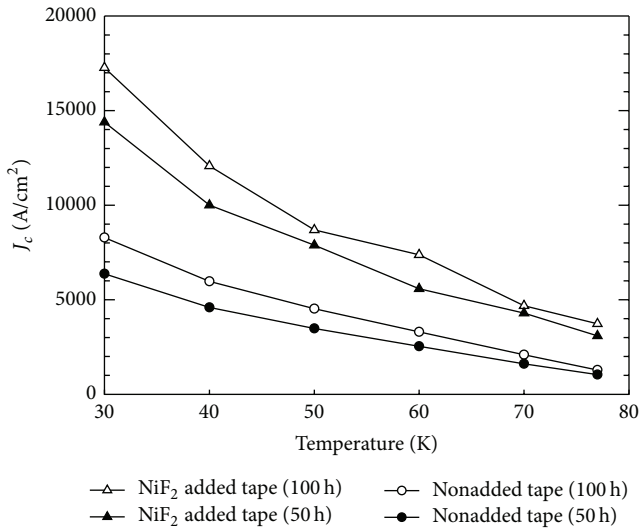

Figure 4: Temperature dependence of critical current density, J_c, in zero magnetic fields for nonadded and NiF_2 added Bi-2223 tapes sintered for 50 and 100 h.

fields either parallel $B_\parallel$ or perpendicular $B_\perp$ to the surface of the tape is shown in Figure 5. The J_c of NiF_2 added tapes was higher than the nonadded tapes in both applied field orientations. J_c of all the tapes decreased with increasing field strength due to the destruction of weak links in the tapes under low magnetic fields [12]. Furthermore, the decrease in

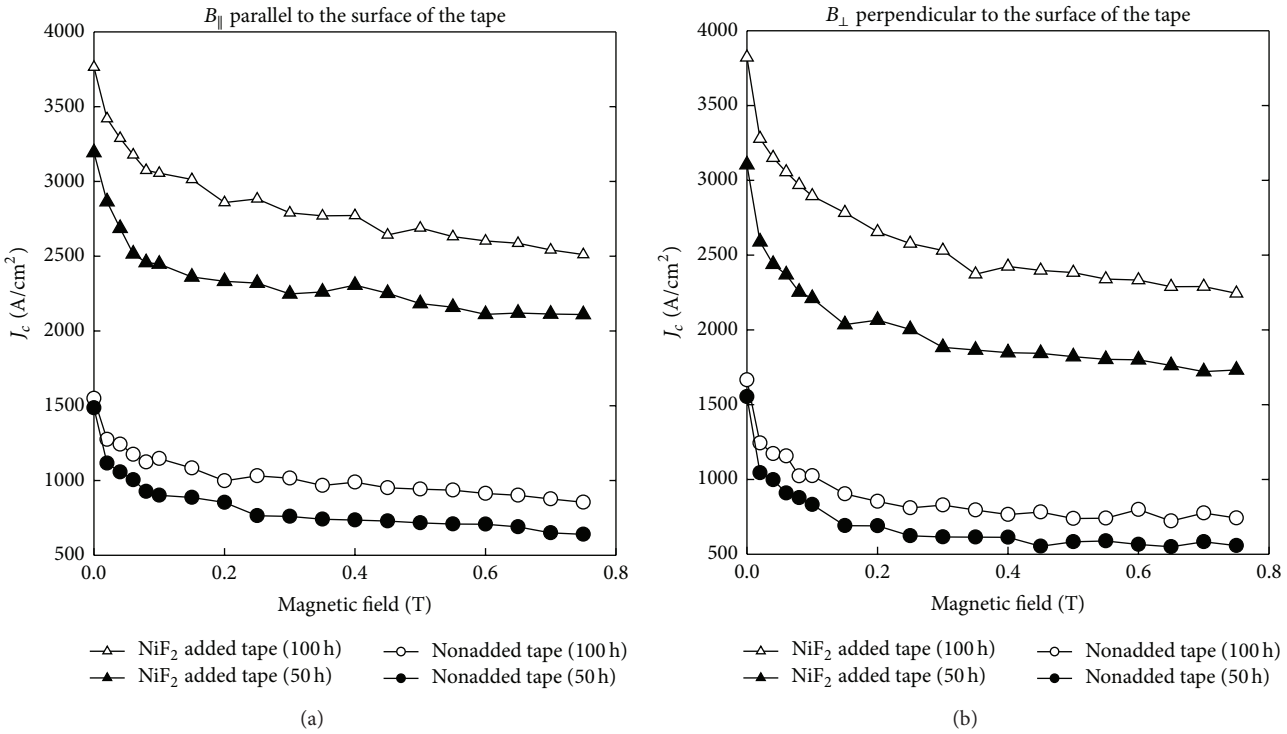

Figure 5: Magnetic field dependence of critical current density, J_c, at 77 K for nonadded and NiF_2 added Bi-2223 tapes sintered for 50 and 100 h.

J_c was slower for tapes under magnetic field applied parallel to the surface of the tape compared to when the field was applied perpendicular to the surface of the tape. This could be explained by the better flux pinning capability behavior along the flat surface of the tapes [18].

4. Conclusion

In conclusion, the effect of antiferromagnetic NiF_2 nanoparticles addition on phase structure, microstructure, and transport critical current density in Bi-2223 superconductor has been investigated. NiF_2 added tapes showed a significant enhancement of J_c compared with the nonadded tapes. This showed that NiF_2 nanoparticles acted as effective pinning centers leading to enhancement of J_c in the Bi-2223 system. A higher J_c was also seen in tapes sintered for 100 h compared with tapes sintered for 50 h due to the improvement in grains connectivity. A sintering time longer than 100 h may enhance J_c even further. A steeper increase in J_c was observed below 60 K and this coincides with the Néel temperature (T_N = 60 K) of nanosized NiF_2. The appearance of antiferromagnetism below 60 K may have enhanced J_c due to strong interaction between the flux lines with the antiferromagnetic NiF_2 nanoparticles.

Conflict of Interests

The authors declare that there is no conflict of interests regarding the publication of this paper.

Acknowledgments

This research was supported by the Malaysian Ministry of Education under Grant no. FRGS/2/2013/SGD2/UKM/01/1 and Universiti Kebangsaan Malaysia under Grant no. UKM-DPP-2014-055.

References

[1] D. Larbalestier, "Superconductor flux pinning and grain boundary control," *Science*, vol. 274, no. 5288, pp. 736–737, 1996.

[2] D. J. Bishop, P. L. Gammel, D. A. Huse, and C. A. Murray, "Magnetic flux-line lattices and vortices in the copper oxide superconductors," *Science*, vol. 255, no. 5041, pp. 165–172, 1992.

[3] N. A. Hamid and R. Abd-Shukor, "Effects of TiO_2 addition on the superconducting properties of Bi-Sr-Ca-Cu-O system," *Journal of Materials Science*, vol. 35, no. 9, pp. 2325–2329, 2000.

[4] M. Annabi, A. M'chirgui, F. Ben Azzouz, M. Zouaoui, and M. Ben Salem, "Addition of nanometer Al_2O_3 during the final processing of (Bi,Pb)-2223 superconductors," *Physica C*, vol. 405, no. 1, pp. 25–33, 2004.

[5] Z. Y. Jia, H. Tang, Z. Q. Yang, Y. T. Xing, Y. Z. Wang, and G. W. Qiao, "Effects of nano-ZrO_2 particles on the superconductivity of Pb-doped BSCCO," *Physica C: Superconductivity and its Applications*, vol. 337, no. 1, pp. 130–132, 2000.

[6] I. H. Gul, F. Amin, A. Z. Abbasi, M. Anis-ur-Rehman, and A. Maqsood, "Effect of Ag_2CO_3 addition on the morphology and physical properties of Bi-based (2223) high-T_c superconductors," *Physica C: Superconductivity and its Applications*, vol. 449, no. 2, pp. 139–147, 2006.

[7] I. F. Lyuksyutov and D. G. Naugle, "Frozen flux superconductors," *Modern Physics Letters B*, vol. 13, no. 15, pp. 491–497, 1999.

[8] W. Kong and R. Abd-Shukor, "Enhanced electrical transport properties of nano $NiFe_2O_4$-added $(Bi_{1.6}Pb_{0.4})Sr_2Ca_2Cu_3O_{10}$ superconductor," *Journal of Superconductivity and Novel Magnetism*, vol. 23, no. 2, pp. 257–263, 2010.

[9] R. Abd-Shukor and W. Kong, "Effect of magnetic nanoparticles Fe3O4 on the transport current properties of Bi-Sr-Ca-Cu-O superconductor tapes," *Journal of Applied Physics*, vol. 105, no. 7, Article ID 07E311-2, 2009.

[10] H. L. Anderson, Ed., *A Physicist's Desk Reference*, American Institute of Physics, New York, NY, USA, 2nd edition, 1989.

[11] D. H. Lee, K. J. Carroll, S. Calvin, S. Jin, and Y. S. Meng, "Conversion mechanism of nickel fluoride and NiO-doped nickel fluoride in Li ion batteries," *Electrochimica Acta*, vol. 59, pp. 213–221, 2012.

[12] M. Ismail, R. Abd-Shukor, I. Hamadneh, and S. A. Halim, "Transport current density of Ag-sheathed superconductor tapes using Bi-Sr-Ca-Cu-O powders prepared by the co-precipitation method," *Journal of Materials Science*, vol. 39, no. 10, pp. 3517–3519, 2004.

[13] Q. Y. Hu, H. K. Liu, and S. X. Dou, "Formation mechanism of high-T_c and critical current in $(Bi,Pb)_2Sr_2Ca_2Cu_3O_{10}$/Ag tape," *Physica C: Superconductivity*, vol. 250, no. 1-2, pp. 7–14, 1995.

[14] R. K. Nkum and W. R. Datars, "Weak link in ceramic In-doped Bi-Pb-Sr-Ca-Cu-O," *Superconductor Science and Technology*, vol. 8, no. 11, pp. 822–826, 1995.

[15] N. A. A. Yahya and R. Abd-Shukor, "Effect of nano-sized PbO on the transport critical current density of $(Bi_{1.6}Pb_{0.4}Sr_2Ca_2Cu_3O_{10})$/Ag tapes," *Ceramics International*, vol. 40, no. 4, pp. 5197–5200, 2014.

[16] N. A. A. Yahya and R. Abd-Shukor, "Electrical transport properties of $(Bi_{1.6}Pb_{0.4}Sr_2Ca_2Cu_3O_{10})$/Ag tapes with different nano-sized MgO," *Advances in Condensed Matter Physics*, vol. 2013, Article ID 821073, 5 pages, 2013.

[17] A. Agail and R. Abd-Shukor, "Effect of different nanosized NiO addition on Ag-sheathed $(Bi_{1.6}Pb_{0.4})Sr_2Ca_2Cu_3O_{10}$ superconductor tapes," *Journal of Superconductivity and Novel Magnetism*, vol. 27, no. 5, pp. 1273–1277, 2014.

[18] F. Feng, T.-M. Qu, C. Gu et al., "Comparative study on the critical current performance of Bi-2223/Ag and YBCO wires in low magnetic fields at liquid nitrogen temperature," *Physica C*, vol. 471, no. 9-10, pp. 293–296, 2011.